Decentralized Reactive Power Sharing and Frequency Restoration in Islanded Microgrid

M. Kosari, *member, IEEE*, S. H. Hosseinian

***Abstract*—P-f and Q-V droop methods are the most common decentralized control methods in islanded microgrid. Although with the P-f droop method an accurate active power sharing can be achieved among distributed energy resources (DERs), by Q-V droop, the reactive power sharing among DERs often deteriorates due to its highly dependence on the power line impedances and the local load. Variation of frequency and voltage by load changes is another challenge in droop control method. In this paper a new autonomous control method is proposed to share reactive power among DERs accurately and restore frequency of a microgrid. The proposed method does not require any communication link and so maintains reliability and simplicity of network. The synchronizing among DERs is obtained by load change detection which is accomplished by wavelet transform. The method operation principle is explained and analyzed. Simulation results are presented to validate the effectiveness of the proposed method.**

***Index Terms*—Decentralized control, droop control, frequency restoration, reactive power sharing, wavelet transform.**

NOMENCLATURE

ω_0	Microgrid nominal frequency
ω_i	ith DER frequency
$\Delta\omega$	Frequency deviation of microgrid for ΔP_l
$\Delta\omega_i$	ith DER locally frequency deviation form ω_0
$\Delta\omega_i(t)$	$\Delta\omega_i$ time function
$\delta\omega_i$	ith DER control term for frequency restoration
V_0	Microgrid nominal voltage
V_i	ith DER output voltage
V_{pcc}	Point of common coupling voltage
ΔV_i	Difference between ith DER voltage and V_{pcc}
P_i	ith DER active power
P_{ir}	ith DER power rating
ΔP_l	Load change value
ΔP_i	Active power contribution of ith DER for ΔP_l
$P_{i,ave}$	Average active power block output of ith DER
Q_i	ith DER reactive power
$Q_{i,local}$	ith DER local load reactive power
N	Number of DER
m_i	ith DER P-f droop curve slope
n_i	ith DER Q-V droop curve slope
k	Constant for changing of frequency restoration rate
K	Equation constant between ΔV_i and Q_i
k_q	Reactive power term coefficient
k_I	Integral gain coefficient
τ_r	Restoration time constant
G	Soft compensation gain
T	Time duration for dynamic suspend

I. INTRODUCTION

MICROGRID is formed when distributed energy resources (DERs) such as photovoltaic, fuel cells, wind turbines, microturbines, etc. are clustered to offer many advantages. The control of the formed microgrid can be centralized where a control center by gathering information from the network and sending command to DERs controls the microgrid. But in some situations where communication links are not viable, the droop control schemes as decentralized control is more appropriate. The droop control is a proportional power sharing among the DERs based on their respective kVA ratings [1]-[5]. However, the droop control method as the decentralized control strategy can operate autonomously without any communication link, and therefore increases reliability and simplicity, but it encounters some challenges and drawbacks.

Although an accurate active power sharing can be achieved among DERs with frequency droop control, the reactive power sharing under the voltage droop control is highly dependent on the output filter impedance of DER interface converter, the local load and power line impedances, and so, this approach for reactive power sharing is often lead to error. Consequently, the problem of reactive power sharing in islanded microgrids has received considerable attention in the literature and many control techniques have been developed to address this issue [6]-[15].

In [6] a method has been proposed based on additional control signal injection to improve the reactive power sharing accuracy. Overlaying such an AC voltage signal may reduce the quality of the output voltage and line current. A comprehensive treatment of the virtual impedance concept to mitigate errors in reactive power sharing is presented by [7]-[9]. Since the local loads have significant effect on reactive power sharing, an algorithm with considering both impedance voltage drop effect and DER local load effect was proposed in [10]. The method works by estimating the impedance voltage drops, so the error in estimation causes the method does not work well and accurately. [11] proposes a $Q-\dot{V}$ droop control method, where $\dot{V}$ represents the rate of change of the voltage magnitude. The method is decentralized that does not need communication link, but does not completely remove reactive power sharing error. In [12] the reactive power control error obtains through injecting small active power disturbances, which is activated by the low-bandwidth synchronization signals and at the same time, a slow integration term for reactive power sharing error elimination is added to the conventional reactive power droop control. Considering no change in load in the activation time duration and need for low bandwidth link are the main drawbacks of the method. In [13], the method improves the reactive power sharing by changing the voltage bias on the basis of the conventional droop control, which is activated by a sequence of synchronization events through the communication network. [14] illustrated the central control strategy to improve reactive power sharing and decrease voltage harmonic distortion in an islanded single phase microgrid. A distributed secondary control strategy is proposed in [15], that every DER by using the measurements of other DERs in each sample time can produce appropriate control signal to control frequency, voltage and reactive power.

Some of methods mentioned above (centralized and Distributed method) need a communication link so they are expensive and decrease reliability of microgrid. Also loss of communication link makes some of these methods to work incorrectly, especially in centralized method microgrid encounters an unstable situation. In a decentralized method, reactive power sharing cannot be achieved completely since a local variable voltage is used in control strategy that is not equal in all DERs.

Another challenge of droop method is variation of frequency and voltage by load changing in the microgrid. In [16]-[18] restoration of frequency and voltage is presented as the secondary control level in a hierarchical control of the microgrid. In these methods the frequency and voltage deviation from the nominal value is determined in the central control and then transmitted to DERs in the microgrid to restore them. Hence the control of the microgrid is supposed to be centralized in these methods too.

This paper presents a new decentralized control method that completely shares reactive power and also restores frequency to nominal value. The proposed method needs DER synchronization to start simultaneously in all of them. For removing any dependency on communication link in the proposed method and so maintaining the autonomy, simplicity and reliability of system, the DER synchronization should be done without any communication link. Hence new decentralized synchronization approach is proposed that accomplishes locally in each DER by detection of load change time in the microgrid. In addition to communication removing, another advantage of the locally load change detection, is the ability of stopping the proposed method if any load change is occurred during the process. This advantage did not mention in the previous studies and if load change is occurred during some of them, their methods will be failed. So they assume that load changing does not occur during their method which is not a correct assumption in real world because the microgrid load changes frequently and randomly can occur during the method.

The remaining of the paper is organized as follows. Section II begins by introducing the conventional power–frequency (P−f) and reactive power–voltage (Q−V) droop control. Section III explains the frequency deviation, not proper sharing in reactive power and proposed method. Synchronizing method is explained in section IV. Finally, the simulation result and conclusion are given in section V and VI respectively.

II. Frequency and Voltage Droop Control

In general, for a small change in the bus voltage magnitude, the active power at the bus does not change appreciably. On the other hand, for a small change in the bus phase angle, the reactive power does not change appreciably, especially when the two buses are separated by a dominant inductive branch. These dependencies are the main reason for using droop method. With these assumptions, the active power of DER unit can be controlled by changing the DER output frequency that varies the phase angle dynamically and the DER reactive power can be controlled by changing the DER output voltage magnitude [1]-[5].

The relation between active power and frequency is given as:

$$\omega_i = \omega_0 - m_i P_i \tag{1}$$

where ω_0 is the nominal system frequency (typically 50 or 60 Hz), ω_i is the operating frequency set point, m_i is the slope of droop curve and P_i is the active power loading of ith DER unit. If the slopes are chosen such that:

$$m_1 P_{1r} = m_2 P_{2r} = \cdots = m_N P_{Nr} \tag{2}$$

where P_{ir} is the rating of ith DER unit and N is the number of DER units, then the DER units share the total load on the microgrid in proportion to their power ratings [2]. This power sharing is independent of number of DER unit actually connected to the microgrid and does not need any data communication. In a similar manner, the $Q-V$ droop characteristic for tuning of output voltage and reactive power control of each DER is given as:

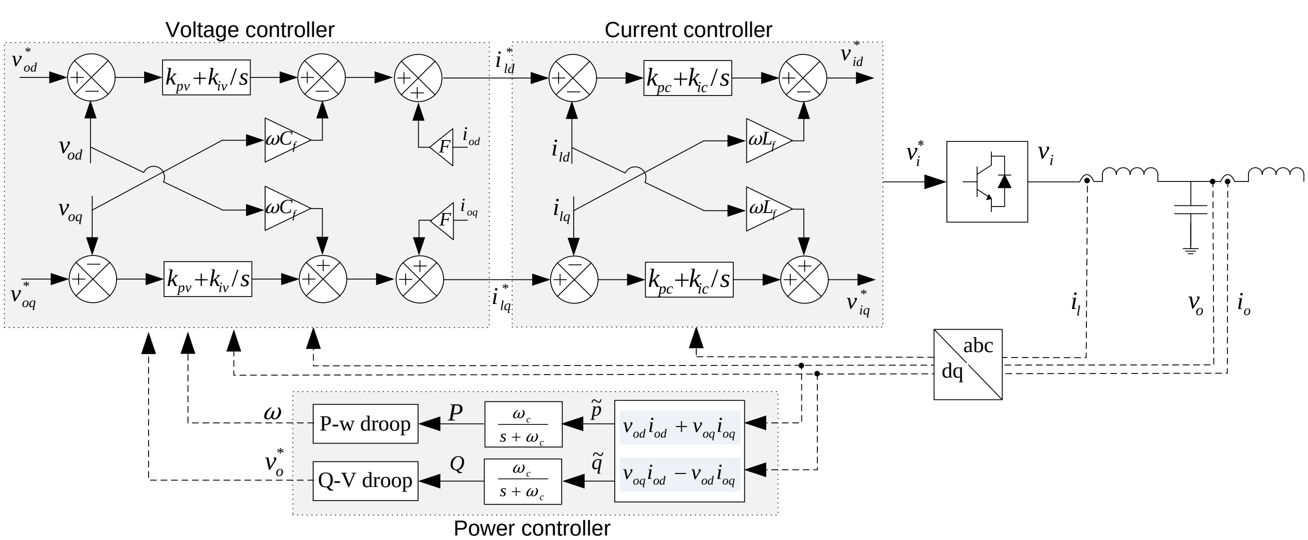

Fig. 1. The DER unit control block diagram

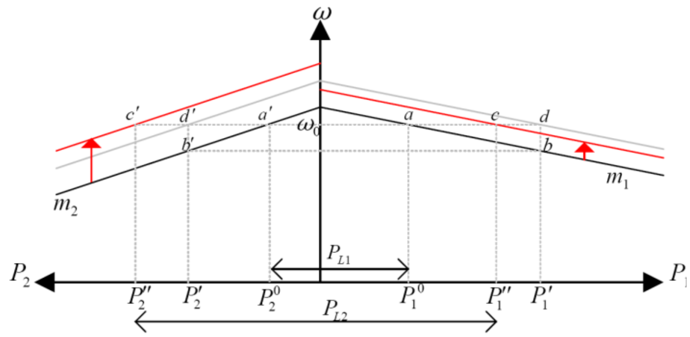

Fig. 2. Effect of not equal droop curve moving on active power sharing of two DER units

$$V_i = V_0 - n_i Q_i \tag{3}$$

where V_0 is the nominal system voltage, V_i is the magnitude of output voltage, n_i is the slope of droop curve and Q_i is the reactive power of the ith DER.

Fig. 1 shows the typical DER control block diagram. The output current and voltage are fed back and transformed into the synchronous reference frame. The output active and reactive power are calculated and then filtered by a low-pass filter [19]. The resulting P and Q are applied to the droop controller to produce the frequency ω and the voltage magnitude V. Then, the voltage reference of converter v_o^* is synthesized in the synchronous reference frame by ω and V. The voltage reference v_o^* then applied to voltage controller and current controller, to produce the pulse width modulation commands of the converter [19].

III. Frequency Deviation, Reactive Power Sharing Error and Proposed Method

A. Frequency deviation in droop control and frequency restoration process (FRP)

Equation (1) implies that the overall system frequency will change by changing the loads. If the m_i slopes of N DERs connected to the microgrid are chosen by (2), for a total load change ΔP_l, the active power contribution of ith DER and the steady-state frequency deviation of microgrid are calculated by [2]:

$$\Delta P_i = \frac{\Delta P_l}{m_i \sum_{j=1}^{N} \frac{1}{m_j}} \tag{4}$$

$$\Delta\omega = \frac{\Delta P_l}{\sum_{j=1}^{N} \frac{1}{m_j}} \tag{5}$$

Fig. 2 shows this situation for the two-DER that for simplicity the droop curves are shown back to back. In this figure, points *a* and *a´* show the condition before a load change, with nominal operating frequency ω_0. After load changing, from P_{L1} to P_{L2}, the operating points shift to *b* and *b´*, which have a lower operating frequency. To have a steady-state operating frequency which is independent of load and at the same time ensures correct active power sharing, the droop characteristics have to be shifted up equally between DERs to pass through points *d* and *d´*. For this shifting, one process which is named frequency restoration process (FRP) should be executed to restore the frequency to its nominal value ω_0. In (1) to perform the FRP, control term $\delta\omega_i$ is added as follow:

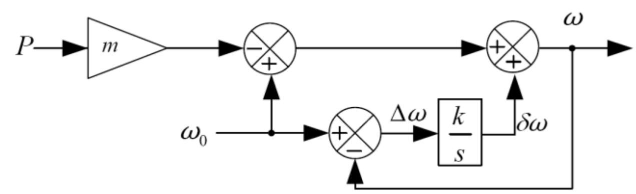

Fig. 3. Frequency restoration method block diagram.

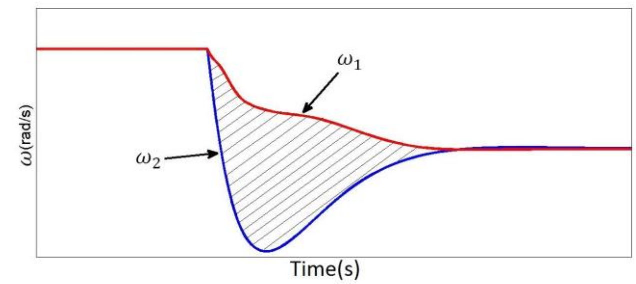

Fig. 4. Dynamic respond of two DER units, the product of hatch area with k constant is the difference in vertical moving of two DER units.

$$\omega_i = \omega_0 + \delta\omega_i - m_i P_i \tag{6}$$

Refering to (6), for the frequency setting ω_i to be equal to the nominal frequency ω_0, the $\delta\omega_i$ must be equal to $m_i P_i$. Thus, the $\delta\omega_i$ is modified so that in the steady state, $\delta\omega_i = m_i P_i$. To achieve this, $\delta\omega_i$ is changed at the following rate:

$$\frac{d(\delta\omega_i)}{dt} = k\Delta\omega_i \tag{7}$$

where $\Delta\omega_i$ are locally measured frequency errors as:

$$\Delta\omega_i = \omega_0 - \omega_i \tag{8}$$

and the k is a constant value and determines the overall rate of frequency restoration. If the changing rate of $\delta\omega_i$ is chosen as above, then the dynamics of the frequency error are determined by the following simple analysis from (1):

$$\frac{d}{dt}(\Delta\omega_i) = \frac{d(\delta\omega_i)}{dt} = k\Delta\omega_i \tag{9}$$

The solution of (9) is:

$$\Delta\omega_i(t) = \Delta\omega\, e^{-t/\tau_r} \tag{10}$$

$$\tau_r = -\frac{1}{k m_i P_{ir}} \tag{11}$$

Equations (10) and (11) indicate that the frequency error decays exponentially to zero, at a rate determined by the restoration time constant τ_r, which depends on the gain k. The frequency restoration method base on laplace transform of (6) and (7) is shown schematically in the control block diagram of Fig. 3.

If the shifted up occurs unequally, the active power sharing encounters a sustained error. For example, suppose for a two DER shown in Fig. 2, second DER is moved more than first DER, results in point c and c´ and variation of active power sharing between two DERs, first DER power supplied decreases from P_1' to P_1'' and second DER power supplied increase from P_2' to P_2''. Vertical moving value of each DER ($\delta\omega_i$) are determined by integral of $\Delta\omega_i$ as shown in Fig. 3. Since the dynamic response of each DER is different especially in the early time of load changing the $\Delta\omega_i$ are different in DERs, and it makes the $\delta\omega_i$ unequal. For example, Fig. 4 shows dynamic response of two DERs and the product of hatched area at k constant is the difference in vertical moving of the two DERs. To decrease the

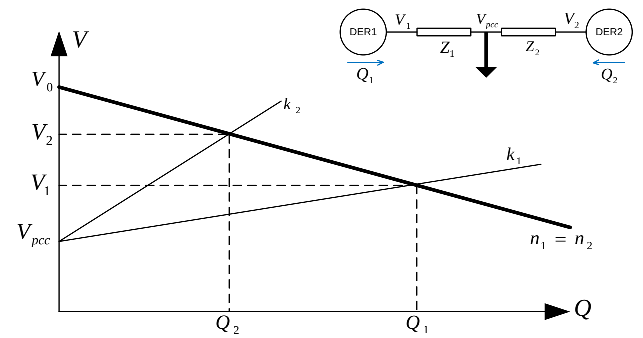

Fig. 5. Effect of feeder impedance on reactive power sharing of two equal rating DERs ($n_1 = n_2$). The second DER has larger feeder impedance.

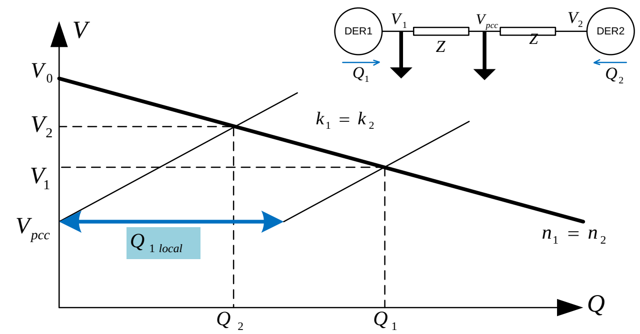

Fig. 6. Effect of local load on reactive power sharing of two equal rating DERs ($n_1 = n_2$). The first DER has local load $Q_{1\ local}$ on terminal output and Feeder impedances are equal ($k_1 = k_2$).

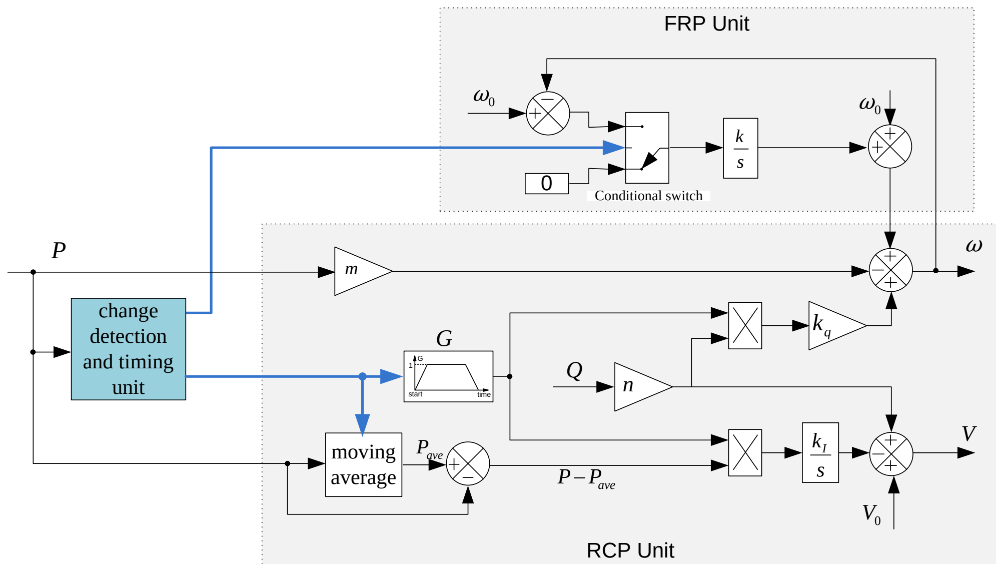

Fig. 7. The RCP and FRP block diagram.

effect of this inequality in the DERs, the k constant should be decreased, but this action does not totally remove the error and also increases restoration time constant τ_r based on (11). In order to restore frequency accurately without any error, the $\delta\omega_i$ must be equal in all DERs. For this, FRP should be started at the same time in all DERs and after smoothing the dynamic response.

B. *Inaccuracy of Reactive Power Sharing Control*

Although, an accurate active power sharing can be achieved among DERs with the P-f droop control, the reactive power sharing under the Q-V droop control is often affected by the voltage drops on DER feeders and the offset of DER local loads. A general voltage drop relationship can be obtained by [10]:

$$V_i = V_{pcc} + \frac{R}{V_{pcc}} P_i + \frac{X}{V_{pcc}} Q_i \quad (12)$$

where V_i and V_{pcc} are the DER and the point of common coupling (PCC) voltage magnitude, $P_i + jQ_i$ is the power supplied from DER and $R + jX$ is the line feeder impedance between DER and PCC. To make the discussion easier, the feeder resistance is ignored, although the effect of resistance can be compensated [10]. So (12) will be as follow:

$$\Delta V_i = V_i - V_{pcc} = \frac{X}{V_{pcc}} Q_i = K Q_i \quad (13)$$

This equation shows the relation between voltage magnitude difference (between DER output voltage and PCC voltage) and DER output reactive power. Since the V_{pcc} is limited to vary in a small range (e.g., ±10%) and the inductance between two voltages is normally constant, it is reasonable to assume K as a constant slope. To illustrate the reactive power error by line impedance, suppose two equal power rating DER units supply the load on the microgrid and therefore they should be equal in power sharing. The second DER has the larger feeder impedance and so larger K slope. So as shown in Fig. 5 the reactive power supplied Q_2 is not the same as Q_1 and is smaller than it.

Now consider the effect of local load on reactive power sharing. Since in presence of local load, the difference of the power supplied by DER and local load is transferred toward the PCC, the local load introduces an offset on the reactive power in (12). It means that even if DER output voltage terminal V_i is the same as V_{pcc}, the reactive power supplied by DER is equal to local load reactive power ($Q_{i,local}$). So (13) is changed as:

$$\Delta V_i = K\left(Q_i - Q_{i,local}\right) \quad (14)$$

The effect of local load on reactive power sharing is illustrated in Fig. 6. Suppose two equal power rating DERs supply load on microgrid with the same feeder impedance, but the first DER has local load on output terminal. In this case voltage drop starting point is shifted to right by local load offset $Q_{1,local}$ and so the reactive power generated by $Q_1$is bigger than Q_2.

C. Proposed reactive power sharing and frequency restoration

At the steady state, the frequency of the microgrid is unique and therefore active power is shared accurately by P-f droop control. This concept can be used to remove the error of reactive power sharing during a process named reactive power compensation process (RCP). It means that during RCP the frequency plays the key role to link DERs together. In the RCP instead of (1) and (2) the following droop control is used:

$$\omega_i = \omega_0 - m_i P_i + G\, k_q \left(n_i\, Q_i\right) \tag{15}$$

$$V_i = V_0 - n_i Q_i + \frac{k_I}{s} G\left(P_i - P_{i,ave}\right) \tag{16}$$

Where k_q and k_I are the reactive power term coefficient and integral gain respectively, which are selected to be equal for all DERs, G is soft compensation gain to minimize the power oscillation during compensation process,(the G contains an increasing ramp at the beginning and a decreasing ramp at the end of the compensation) [12]. $P_{i,ave}$ is the output of an average active power block in ith DER to filter out power ripple. This block prevents updating $P_{i,ave}$ at the starting moment of the compensation process and holds the last $P_{i,ave}$ to be used in compensation process. The added reactive power term in (15) imposes the reactive power sharing error in the P-f droop control and active power. In this case, the difference between disturbed P_i and $P_{i,ave}$ is the reactive power sharing error. This term is calculated by integrating of (16). During transient the integral term eliminates this error and finally P_i will be equal to $P_{i,ave}$. Since at the final the frequency is unique and same in all DERs, the last term of (15) must be equal in all the DERs, therefore:

$$n_1 Q_1 = n_2 Q_2 = \cdots = n_N Q_N$$

It means that reactive power shared accurately in proportion to power rating. After eliminating the error, the RCP can be ended by decreasing G gain softly to return frequency to the value before starting process. It is worth to say that the RCP should be started and performed in all DERs simultaneously.

Also as stated before, to accurately restore frequency to nominal value FRP should be started simultaneously after smoothing the dynamic response in all DERs. Therefore, the synchronization for simultaneously executing of RCP and FRP in all DERs is very important. If communication link is used in the microgrid the achievement of DERs synchronization will be easy but decreases the simplicity and reliability of the system.

Here a new synchronization method is proposed that without any communication link carry out locally in each DER. Hence by this method not only autonomous operation, simplicity and reliability of microgrid are maintained but also the load can be changed anytime without any problem even during RCP and FRP. If the microgrid load is changed or other phenomena is taken place, the electrical parameters change suddenly. If the change moment can be detected in the each DER, it can be used as the synchronizing signal and the time origin. The change detection method is proposed in the next section.

After any change detection, time duration T must be elapsed to assure that all dynamics are passed. This time duration will be equal for all DER units and can be four times of slowest DERs time constant which is the one with smallest m_i (based on the stability and root locus analysis [19]-[23]). After the time duration the RCP starts. After ending of RCP, the FRP process starts. If before the passing of duration T, another change is taken place, the accounting of T starts from this new load change moment again. If in the RCP/FRP a change is occurred, the RCP/FRP is stopped and the T calculated from the new change point again. RCP should be stopped by switching gain G to zero. The RCP and FRP block diagram are shown in Fig.7.

IV. Change Detection by Wavelet Transform

Wavelets are mathematical functions with time-frequency representation for the analysis of a signal with transient features. The wavelets are scaled and translated copies (known as "daughter wavelets") of a finite-length or fast-decaying oscillating waveform (known as the "mother wavelet"). Usually, the wavelet transform (WT) that is the representation of a function by wavelets is expressed by a multi resolution decomposition algorithm which utilizes the orthogonal wavelet bases to decompose the signal to components under different scales and one can assign a frequency range to each scale component. Each scale component can be studied with a resolution that matches its scale. WT have advantages over traditional fourier transforms for representing functions that have discontinuities and sharp peaks. Also for accurately deconstructing and reconstructing finite, non-periodic and/or non-stationary signals WT is better. The continuous WT for a given signal x(t) at a scale a and translation factor b is expressed by the following integral [24], [25]:

$$W_{a,b}(t) = \frac{1}{\sqrt{|a|}} \int_{-\infty}^{\infty} x(t)\psi\left(\frac{t-b}{a}\right) dt \tag{17}$$

where $\psi(t)$ is the mother wavelet. The coefficients of WT are defined by the following inner product:

$$C(a,b) = \int_0^{\infty} x(t) W'_{a,b}(t) dt \tag{18}$$

In the other expression, WT can be extracted as a series of bandpass filters, containing successive pairs of low-pass and high-pass filters, providing approximate and detailed coefficients. The approximations are the high-scale, low frequency components of the signal produced by filtering the signal by a low-pass filter. The details are produced by filtering the signal through a high-pass filter and are the low-scale, high frequency components of the signal. The detailed coefficients provide vital information for time-localizing transient events at different levels of decomposition.

Detection of signal change by WT is as follow. At each time step a window with determined length containing current time step of signal is constructed, then decomposed by wavelet to approximate and detailed coefficients. In normal pattern of signal, coefficients of details are very low and noisy value but at the time of signal changing they will be so large. This large difference is used for detection of changing moment. So the coefficients are compared with threshold and if it is bigger than threshold the timing process is started. It is worth to say that the coefficients are large only near the change point and then decrease rapidly.

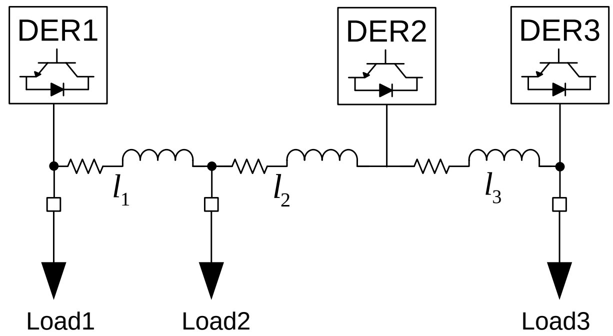

Fig. 8. Circuit configuration for computer simulations.

TABLE I
DETAILED CONTROLBLOCK PARAMETERS [19]

	parameter	value
Output filter	C_f	50 μF
	L_f	1.35 mH
	r_f	0.1Ω
Output impedance	L_c	0.35 mH
	r_{Lc}	0.03Ω
Voltage controller	K_{pv}	0.05
	K_{iv}	390
	F	0.75
Current controller	K_{pc}	10.5
	K_{ic}	16e3
cut-off frequency	w_c	31.41

TABLE II
SYSTEM PARAMETER

nominal voltage	380V (RMS line to line)
nominal frequency	ω=314 rad/s (f=50Hz)
line impedance	l_1=0.4+j0.3Ω l_2=0.2+j0.1Ω l_3=0.2+j0.2Ω
P-f slope droop	$m_1=1\times10^{-4}$ $m_2=0.5\times10^{-4}$ $m_3=1\times10^{-4}$
Q-V slope droop	$n_1=1\times10^{-3}$ $n_2=0.5\times10^{-3}$ $n_3=1\times10^{-3}$
load	load1=4kW+j2kVar load2= 4kW+j2kVar load3= 4kW+j2kVar
k_q	0.05
k_I	0.05
k	10
T (dynamics suspended time)	1s
G (soft compensation gain)	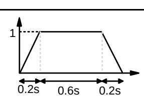

V. SIMULATION STUDY

To validate the effectiveness of the proposed method a networked microgrid model has been established using MATLAB/Simulink. The simulated microgrid is composed of three DER units as shown in Fig. 8. Controlling of each DER unit is as Fig. 1. Detailed control is based on [19] which its control block parameters are given in Table I. Power rating of DER1 and DER3 are 10kVA and power rating of DER2 is 20kVA. The System parameters are given in Table II.

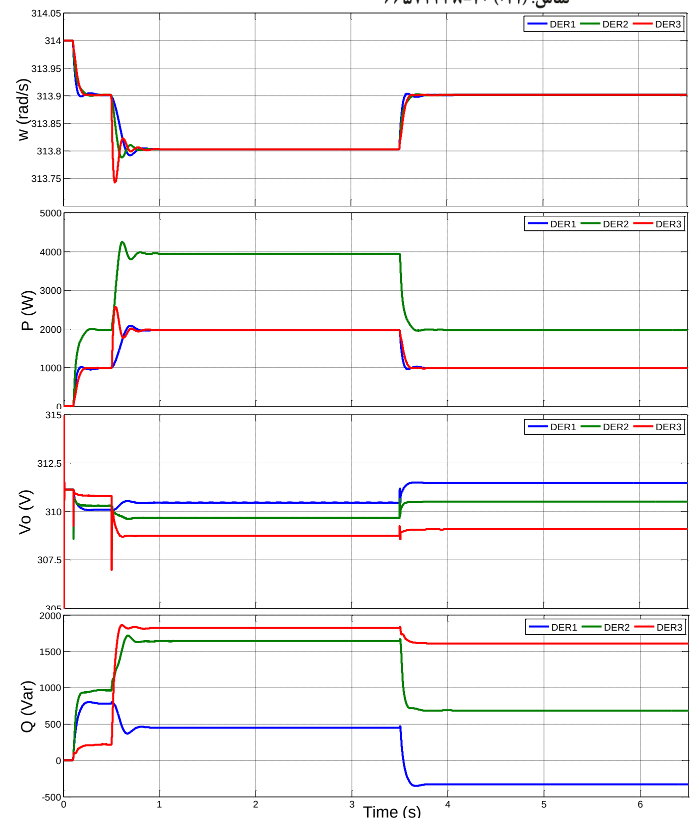

Fig. 9. The frequency, active power, output voltage and reactive power of three DERs without proposed method (load2 is connected at 0.1s and disconnected at 3.5s and load3 is connected at 0.5s).

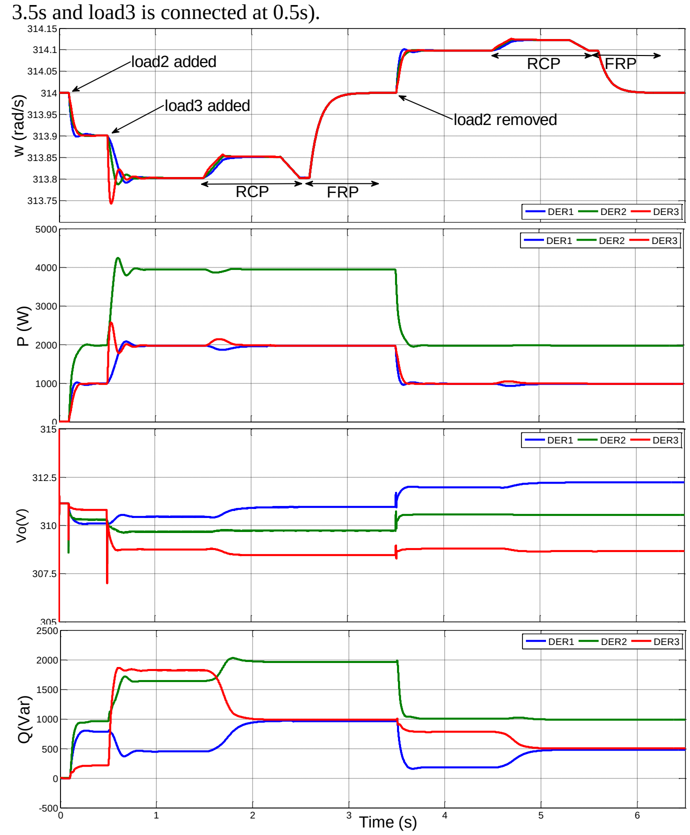

Fig. 10. The frequency, active power, terminal voltage and reactive power of three DERs with proposed method (load2 is connected at 0.1s and disconnected at 3.5s and load3 is connected at 0.5s).

A. *Effectiveness of proposed method*

Suppose that at the first, the proposed method is not used and load2 is connected at 0.1s and disconnected at 3.5s and load3 is connected at 0.5s. The frequency, active power, terminal voltage

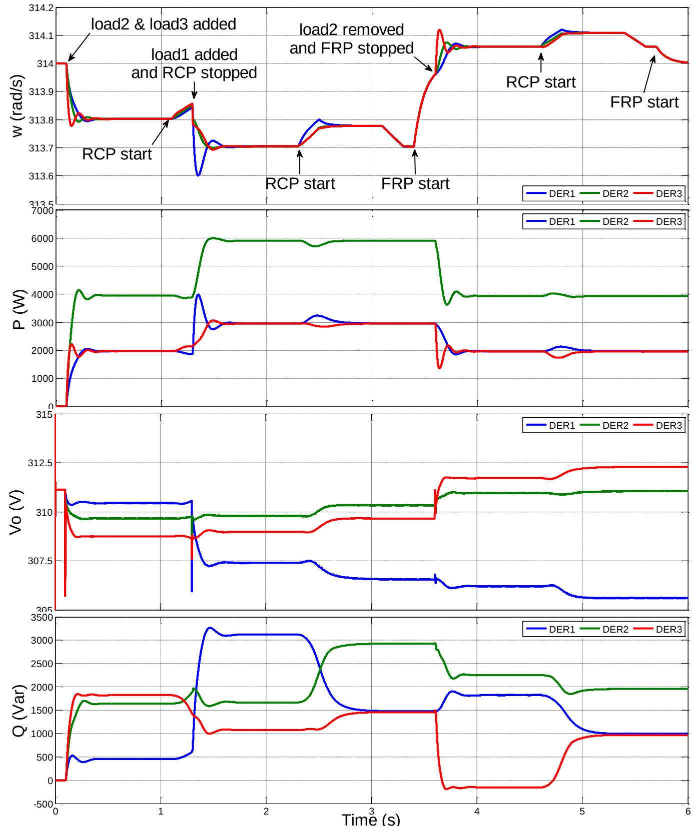

Fig. 11. Effect of load changing in the RCP/FRP. The frequency, active power, terminal voltage and reactive power of three DERs with proposed method when between RCP/FRP load1 at 1.3s is added and load2 at 3.6s is removed.

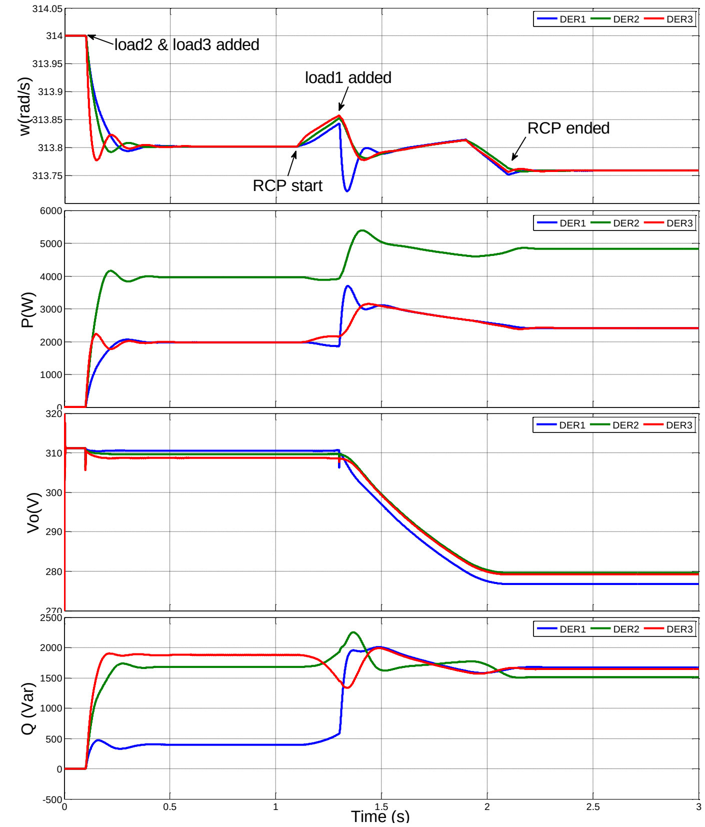

Fig. 12. Effect of load changing on the RCP method of [12]. The frequency, active power, terminal voltage and reactive power of three DERs with method of [12] when load1 at 1.3s between RCP is added.

and reactive powers of the three DERs with this load change scenario are depicted in Fig. 9. It is obvious that the active power is shared accurately among three DERs proportion to nominal rating and P-f droop slope, but the reactive power encounter to unacceptable error. Also the frequency is not fix and changes with load variation.

Now, the proposed method is applied. The frequency, active power, terminal voltage and reactive power of three DERs with the same load change scenario are depicted in Fig. 10. As illustrated in it after load changing the RCP eliminates the reactive power sharing error and the FRP eliminates the frequency deviation. For example when the load2 and load3 are connected and before the starting of RCP/FRP at 1.5s, the reactive power of DERs are Q1=1800 Var, Q2=1595 Var, Q3=590 Var and ω=313.8 rad/s but after RCP/FRP the reactive power of DERs are Q1=1006 Var Q3=987 Var and Q2=1995 Var and ω=314 rad/s. It means approximately Q1 is equal to Q3 and half of Q2, so the reactive power shares accurately among DERs and also frequency is restored to nominal value.

B. *Operation under load changing during compensation process*

To illustrate what happened if the load is changed in the RCP/FRP, this new scenario is executed: load2 and load3 are added at 0.1s, load1 is added at 1.3s and load2 is removed at 3.6s. With elapsed time T=1s after adding load2 and load3, the RCP/FRP is started at 1.1s. But 0.2s later at 1.3s, the next load change is taken place, so the RCP/FRP is stopped by switching gain G to zero. The timing unit is accounted duration time T from this point again and at the 2.3s makes RCP/FRP to be started. At 3.6s when the RCP is ended and FRP is started, the next load change is taken place, so the FRP is stopped and the timing unit is accounted T from this point again and at the 3.6s starts RCP/FRP. Frequency, active and reactive power of DERs during this scenario are shown in Fig. 11.

To show the importance of locally synchronization of DERs, the proposed RCP is compared with method of [12]. In [12] a low band communication link is used to send activation command for starting compensation process in all DERs simultaneously. Moreover of communication link requirement, it assumes that load changing does not occur in the compensation process that is not a correct assumption in real condition because the microgrid load changes frequently and randomly can occur in compensation process. If load is changed in the compensation process, the load change is seen as reactive power error and the method attempts to remove it. In this situation a sustained error is imposed on the active power and voltage of DERs. Hence this unacceptable drawback makes the method of [12] to be impractical in fact. Since only the RCP is considered in [12], the previous scenario until 3s is adequate for comparison. It is supposed that central control in [12] activates process at 1.1s. Since the process ended only when the soft gain G comebacks to zero and it cannot sense load changing moment to stop process at 1.3s, the process continues and attempts to reach active powers (P_i) to its value ($P_{i,ave}$) at 1.1s i.e. the time of starting process. Hence the active power (and the voltage as result of it) encounter sustained error and instead of decreasing to lower value for load removing, its incorrectly increased to $P_{i,ave}$. Fig. 12 shows the frequency, active power, terminal voltage and reactive power of DERs in this situation.

C. Proposed method with unbalanced load

To illustrate performance of proposed method on unbalance load, the system with load1 and load3 is supposed to be in steady state and an unbalanced load (phase A=1500W+j800 Var, phase B=500W+j300Var, phase C=0W+j0Var) in load2 position is added at time 3s. Frequency, active power, terminal voltage and reactive powers of DERs are shown in Fig 13. As seen the RCP/FRP works properly under unbalanced load as well as balanced load.

D. Synchronizing by wavelet transform

To illustrate the performance of WT for the detection of changes that is the basis of synchronizing between DERs in the RCP/FRP, different load change in position of load1 to load3 is accomplished to cover the large value as well as the low value load changes. In here, a window of 64 time steps is analyzed by the tenth order daubechies wavelet (db10). Time, situation, absolute value of detail coefficient before and after load change and the ratio of them are summarized in Table III. Power and absolute detail coefficient value in this case is shown in Fig. 14 and Fig. 15 respectively. Detail coefficients are noisy value and are under 1e-9 before changing of load as seen in the Table III, but as soon as the load change is taken place these coefficient increases significantly. Although the difference in coefficient before and after the load change or ratio of them depends on the load variation value and its position, this difference or ratio is so large that the moment of load change is easily detectable in all DERs. As seen in the Table III, the ratio of coefficient is not less than 1000 even in low load variation. The coefficients in Table III are for the first time step after load change and they become larger in the later time steps. Powerful of method makes it

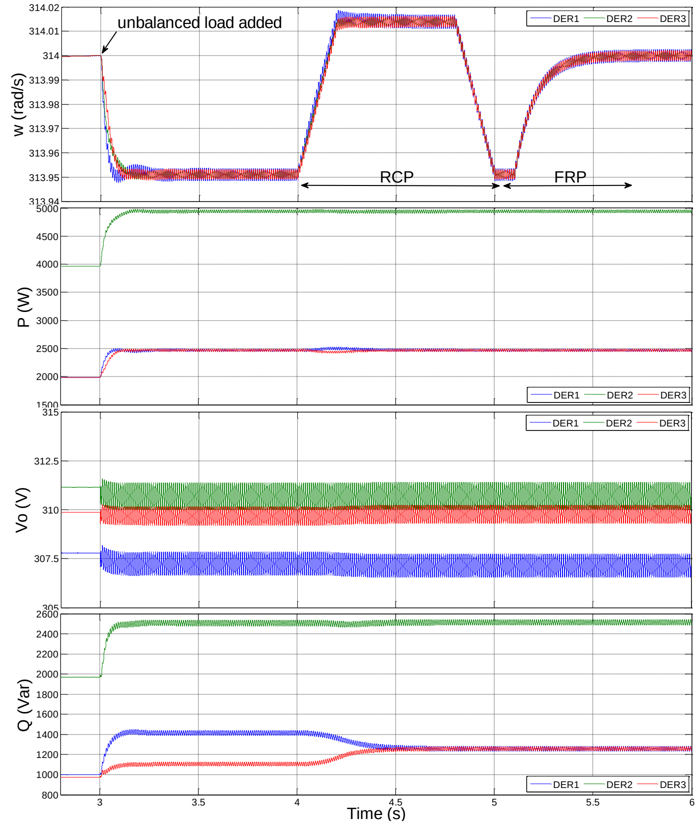

Fig. 13. The frequency, active power, terminal voltage and reactive power of three DERs with proposed method under unbalanced load (system with load1 and load3 is in steady state and unbalanced load is added at 3s).

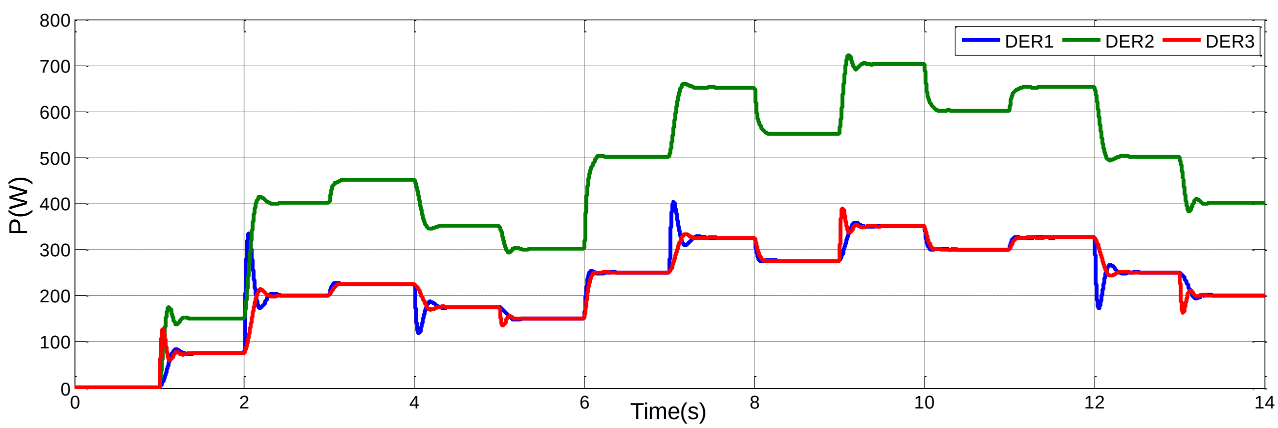

Fig. 14. Active power of three DERs with load change scenario as Table III.

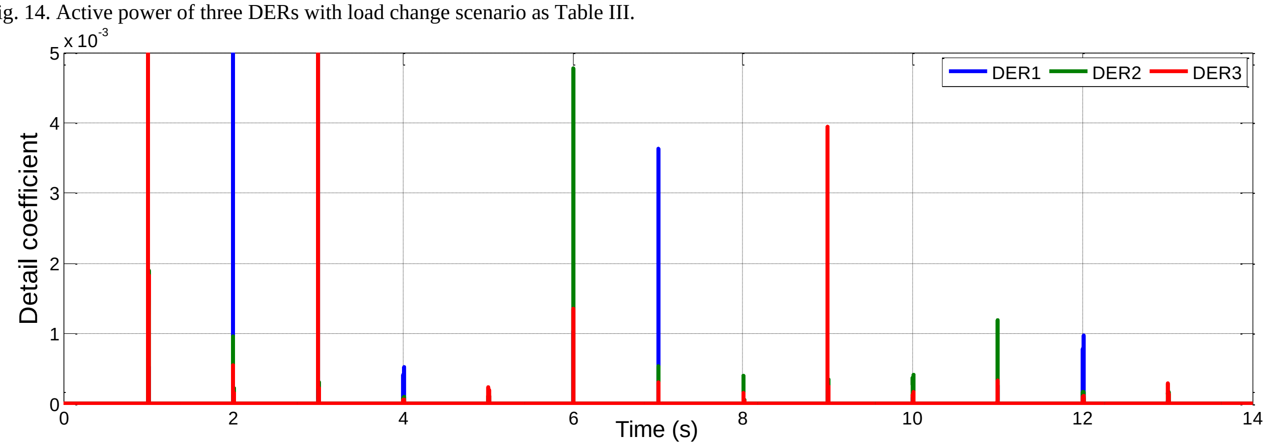

Fig. 15. Detail coefficient of three DERs with load change scenario as Table III.

TABLE III
DETAIL COEFFICIENT OF DER UNIT WITH VARIOUS LOAD CHANGE

Time (Sec.)	Load value P(W)+jQ(var)	Change status	position	DER 1 detail coefficient			DER 2 detail coefficient			DER 3 detail coefficient		
				before	After	ratio	before	after	ratio	before	after	ratio
1	300+j100	Add	Load3	1.4e-16	1.5e-6	1.0e+10	1e-15	4.3e-5	4.30e+10	2.3e-15	6.4e-4	2.7e+11
2	500+j300	Add	Load1	1.1e-12	7.1e-4	6.4e+08	2.1e-12	2.4e-5	1.14e+07	1.1e-12	1.7e-6	1.5e+06
3	j100	Add	Load2	2.9e-12	6.8e-4	2.3e+08	5.7e-12	1.8e-3	3.16e+08	2.8e-12	1.2e-4	4.2e+07
4	200+j100	removed	Load1	3.2e-12	6.2e-5	1.9e+07	6.3e-12	2.1e-6	3.33e+05	3.3e-12	1.4e-7	4.2e+04
5	100+j50	removed	Load3	1.6e-10	2e-6	1.2e+04	4.6e-11	2.7e-6	5.87e+04	3.6e-12	3.3e-6	9.1e+05
6	400+j200	Add	Load2	1.8e-9	1.7e-4	9.4e+04	2.5e-10	4.3e-4	1.72e+06	1.4e-9	3e-5	2.1e+04
7	300+j200	Add	Load1	1.6e-9	4e-4	2.5e+05	4.3e-10	1.3e-5	3.02e+04	2.6e-10	9.4e-7	3.6e+03
8	200+j100	removed	Load2	9.5e-10	1.3e-5	1.3e+04	8.2e-11	3.4e-5	4.15e+05	2.7e-10	2.4e-6	8.8e+03
9	300+j200	Add	Load3	1.3e-10	9.3e-7	7.1e+03	1.4e-9	2.6e-5	1.86e+04	8e-9	3.9e-4	4.8e+04
10	200+j100	removed	Load2	1.1e-9	1.9e-5	1.7e+04	2.2e-9	4.8e-5	2.18e+04	1.3e-9	3.3e-6	2.5e+03
11	100+j50	Add	Load2	3.7e-10	4.2e-5	1.1e+05	5.7e-9	1.1e-4	1.93e+04	2.1e-9	7.6e-6	3.6e+03
12	300+j200	removed	Load1	2e-10	7.9e-4	3.9e+06	9.8e-9	7.6e-5	7.76e+03	3.5e-10	1.2e-6	3.4e+03
13	200+j50	removed	Load3	1.2e-9	1.4e-6	1.1e+03	1.5e-8	1.6e-5	1.07e+03	5.8e-8	2e-4	3.4e+03

suitable for other application that needs DER unit synchronizing in the microgrid.

VI. CONCLUSION

This paper presents a new decentralized method for accurate reactive power sharing and frequency restoration in an islanded microgrid. The proposed method is autonomous and does not require any communication link between DERs units and so maintain simplicity and reliability of system. The basic of synchronizing DERs is the detection of load change moment in each DER that accomplished by the wavelet analysis. The simulation results show the proposed method is very efficient.

VII. APPENDIX

Small-Signal Modeling and Analysis

Small signal analysis method can be applied to investigate the stability and transient performances of DERs during the RCP/FRP. Since the RCP small signal analysis is performed in [12], only the small signal analysis of FRP is investigated in here. For this the state matrix of microgrid is obtained with some modification of microgrid state space model of [19].

As shown in Fig. 1, the DER converter controller is composed of power controller, voltage controller, current controller and output filter. First in the power controller the instantaneous active and reactive power components $\tilde{p}$ and $\tilde{q}$ are calculated from the measured output voltage and output current as:

$$\tilde{p} = v_{od}\, i_{od} + v_{oq}\, i_{oq}\ , \qquad \tilde{q} = v_{oq}\, i_{od} - v_{od}\, i_{oq} \tag{19}$$

then they are passed through low-pass filter to obtain the fundamental component of active and reactive power as:

$$P = \frac{\omega_c}{s+\omega_c}\tilde{p}, \qquad Q = \frac{\omega_c}{s+\omega_c}\tilde{q} \tag{20}$$

where ω_c is the cut-off frequency of low-pass filter. Afterward P and Q are applied to droop controller to generate the reference value for voltage controller. For modeling of FRP, (3) and (6) should be used in droop controller. Also as discuss with more detail in [19], to construct the complete model of DER on a common reference frame, the angle δ is defined for each DER as:

$$\delta = \int \omega - \omega_{com} \tag{21}$$

where ω_{com} is the common reference frame frequency. Now by linearization and rearranging of (3), (6), (7) and (19)-(21), the small signal power controller model can be written in a state space form as:

$$\begin{bmatrix} \Delta\dot{\delta}\omega \\ \Delta\dot{\delta} \\ \Delta\dot{P} \\ \Delta\dot{Q} \end{bmatrix} = A_P \begin{bmatrix} \Delta\delta\omega \\ \Delta\delta \\ \Delta P \\ \Delta Q \end{bmatrix} + B_P \begin{bmatrix} \Delta i_{ldq} \\ \Delta v_{odq} \\ \Delta i_{odq} \end{bmatrix} + B_{P\omega com}\left[\Delta\omega_{com}\right] \tag{22}$$

$$\begin{bmatrix} \Delta\omega \\ \Delta v_{odq}^{*} \end{bmatrix} = \begin{bmatrix} C_{P\omega} \\ C_{Pv} \end{bmatrix} \begin{bmatrix} \Delta\delta\omega \\ \Delta\delta \\ \Delta P \\ \Delta Q \end{bmatrix} \tag{23}$$

where

$$A_P = \begin{bmatrix} -k & 0 & k\,m & 0 \\ 1 & 0 & -m & 0 \\ 0 & 0 & -\omega_c & 0 \\ 0 & 0 & 0 & -\omega_c \end{bmatrix}, \qquad B_{P\omega com} = \begin{bmatrix} 0 \\ -1 \\ 0 \\ 0 \end{bmatrix},$$

$$B_P = \omega_c \begin{bmatrix} 0 & 0 & 0 & 0 & 0 & 0 \\ 0 & 0 & 0 & 0 & 0 & 0 \\ 0 & 0 & I_{od} & I_{oq} & V_{od} & V_{oq} \\ 0 & 0 & -I_{oq} & I_{od} & V_{oq} & -V_{od} \end{bmatrix},$$

$$C_{P\omega} = \begin{bmatrix} 1 & 0 & -m & 0 \end{bmatrix},\ C_{Pv} = \begin{bmatrix} 0 & 0 & 0 & -n \\ 0 & 0 & 0 & 0 \end{bmatrix}.$$

As seen the FRP added state variable $\Delta\delta\omega$ to power controller model. The modeling of voltage and current controller and output filter of DER controller as well as the modeling of microgrid network and load are similar to [19]. So by replacing above power controller model in [19] and following that, the state matrix and eignvalue of microgrid are obtained.

Using the above procedure, a complete model of the test system of Fig. 8 with proposed FRP was obtained. The low frequency modes of system with operation point based of Table I and Table II with load1 and load2 in the connected status are shown in Fig. 16. The response of the system to different active power droop slopes (m) is depicted in Fig. 17. It is obvious that as

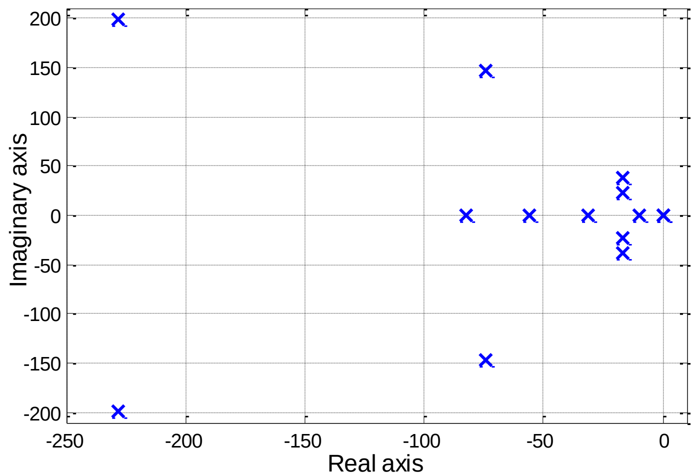

Fig. 16. The low frequency modes of test system with parameter of Table I and Table II with load1 and load2 in the connected status.

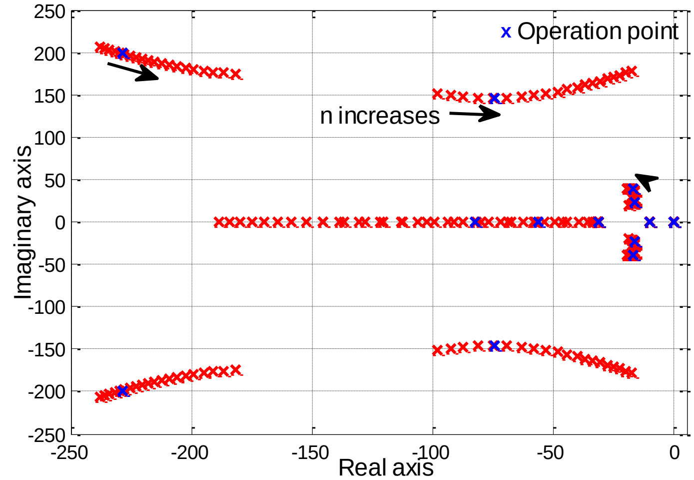

Fig. 18. Trace of low frequency modes of test system as a function of reactive power droop gain: [1e-4, 0.5e-4, 1e-4]<[n_1, n_2, n_3]<[5e-3, 2.5e-3, 5e-3]

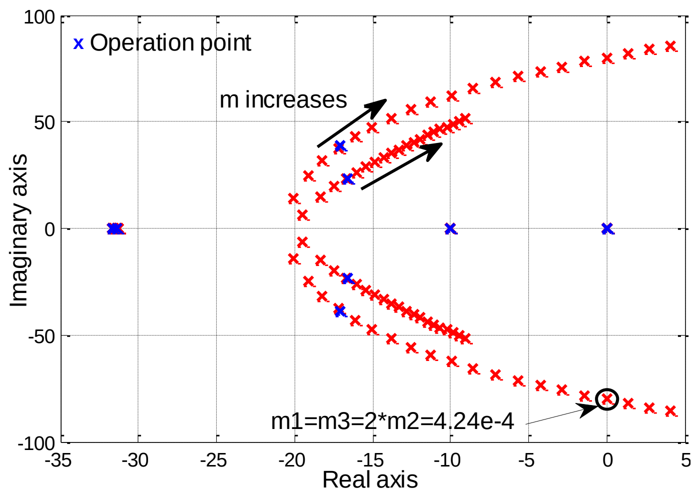

Fig. 17. Trace of dominant modes of test system as a function of active power droop gain: [2e-5, 1e-5, 2e-5]<[m_1, m_2, m_3]<[5e-4, 2.5e-4, 5e-4]

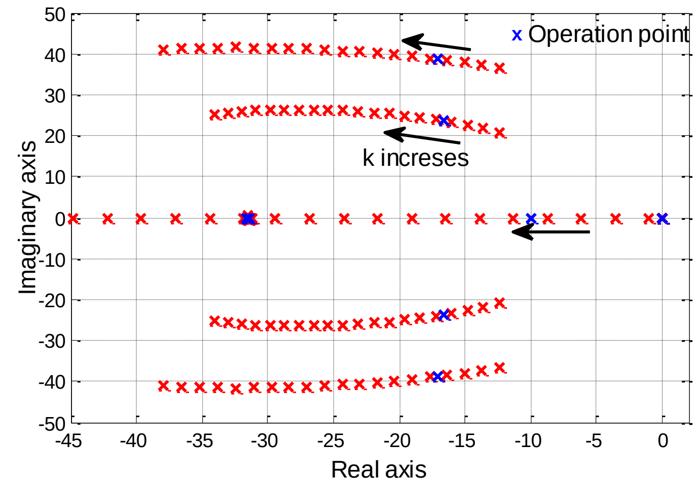

Fig. 19. Trace of dominant frequency modes as a function of integral gain constant of FRP: 1<k<50

m is increased, two dominant modes move towards unstable region making the system more oscillatory and eventually leading to instability. Also the response of the system to variation of reactive power droop slopes (n) and integral gain constant of FRP (k) are depicted in Figs. 18 and 19 respectively. As seen, the increasing of n has not large effect on dominant mode, but it moves other less dominant modes towards unstable region. Increasing of k moves the dominant mode to the left and improves the stability of system as shown in Fig. 19.

REFERENCE

[1] M. C. Chandrokar, D. M. Divan, and R. Adapa, "Control of parallel connected inverters in standalone ac supply systems," *IEEE Trans. Ind.Appl.*, vol. 29, no. 1, pp. 136–143, Jan./Feb. 1993.

[2] M. C. Chandrokar, D. M. Divan, and B. Banerjee, "Control of distributed ups systems," in *Proc. IEEE Power Electron. Spec. Conf.*, Jun., 1994, pp. 197–204.

[3] M. N. Marwali, J.-W. Jung, and A. Keyhani, "Control of distributed generation systems—Part II: Load sharing control," *IEEE Trans. Power Electron.*, vol. 19, no. 6, pp. 1551–1561, Nov. 2004.

[4] K. D. Brabandere, B. Bolsens, J. V. denKeybus, A. Woyte, J. Driesen, and R. Belmans, "A voltage and frequency droop control method for parallel inverters," *IEEE Trans. Power Electron.*, vol. 22, no. 4, pp. 1107–1115, Jul. 2007.

[5] E. Barklund, N. Pogaku, M. Prodanovic, C. Hernandez-Aramburo, and T.C. Green, "Energy management in autonomous microgrid using stability constrained droop control of inverters," *IEEE Trans. Power Electron.*, vol. 23, no. 5, pp. 2346–2352, Sep. 2008.

[6] A. Tuladhar, H. Jin, T. Unger, and K. Mauch, "Control of parallel inverters in distributed AC power system with consideration of line impedance effect," *IEEE Trans. Ind. Appl.*, vol. 36, no. 1, pp. 131–138, Jan./Feb. 2000.

[7] W. Yao, M. Chen, J. Matas, J. M. Guerrero, and Z.-M. Qian, "Design and analysis of the droop control method for parallel inverters considering the impact of the complex impedance on the power sharing," *IEEE Trans. Ind. Electron.*, vol. 58, no. 2, pp. 576–588, Feb. 2011.

[8] J. M. Guerrero, J. Matas, L. G. de Vicu˜na, M. Castilla, and J. Miret, "Decentralized control for parallel operation of distributed generation inverters using resistive impedance," *IEEE Trans. Ind. Electron.*, vol. 54, no. 2, pp. 994–1004, Apr. 2007.

[9] J. M. Guerrero, L. G. de Vicu˜na, J. Matas, M. Castilla, and J. Miret, "Output impedance design of parallel-connected UPS inverters with wireless load-sharing control," *IEEE Trans. Ind. Electron.*, vol. 52, no. 4, pp. 1126–1135, Aug. 2005.

[10] Y. W. Li and C. Kao, "An accurate power control strategy for power electronics-interfaced distributed generation units operation in a low voltage multibus microgrid," *IEEE Trans. Power Electron.*, vol. 24, no. 12, pp. 2977–2988, Dec. 2009.

[11] C. T. Lee, C. C. Chu and P. T. Cheng, "A New Droop Control Method for the Autonomous Operation of Distributed Energy Resource Interface Converters," *IEEE Trans. Power Electron.*, vol. 28, no. 4, pp. 1980–1993, Apr. 2013.

[12] J. He and Y. W. Li, "An Enhanced Microgrid Load Demand Sharing Strategy," *IEEE Trans. Power Electron.*, vol. 27, no. 9, pp. 3984–3995, Sep. 2012.

[13] H. Han, Y. Liu, Y. sun, M Su and J. M. Guerrero, "An Improved Droop Control Strategy for Reactive Power Sharing in Islanded Microgrid," *IEEE Trans. Power Electron.*, DOI 10.1109, early access 2014.

[14] A. Micallef, M Apap, C. S. Staines, J. M. Guerrero and J. C. Vasquez, "Reactive Power Sharing and Voltage Harmonic Distortion Compensation of Droop Controlled Single Phase Islanded Microgrids," *IEEE Trans. Smart Grid*, vol. 5, no. 3, pp. 1149–1158, May. 2014.

[15] Q. Shafiee, J. M. Guerrero and J. C. Vasquez, "Distributed Secondary Control for Islanded Microgrids-A Novel Approach," *IEEE Trans. Power Electron.*, vol. 29, no. 2, pp. 1018–1031, Feb. 2014.
[16] J. M. Guerrero, J. C. Vasquez, J. Matas, L. G. de Vicuna, and M. Castilla, "Hierarchical control of droop-controlled AC and DC microgrids: A general approach toward standardization," *IEEE Trans. Ind. Electron.*, vol. 58, no. 1, pp. 158–172, Jan. 2011.
[17] A. Bidram and A. Davoudi, "Hierarchical structure of microgrids control system," *IEEE Trans. Smart Grid*, 2012, vol. 3, no. 4, pp. 1963–1976, Dec. 2012.
[18] Y. A. R. I. Mohamed and A. A. Radwan, "Hierarchical control system for robust microgrid operation and seamless mode transfer in active distribution systems," *IEEE Trans. Smart Grid*, vol. 2, pp. 352–362, Jun. 2011.
[19] N. Pogaku, M. Prodanovic, and T. C. Green, "Modeling, analysis and testing of autonomous operation of an inverter-based microgrid," *IEEE Trans. Power Electron.*, vol. 22, no. 2, pp. 613–625, Mar. 2007.
[20] E. A. A. Coelho, P. C. Cortizo, and P. F. D. Garcia, "Small-signal stability for parallel-connected inverters in stand-alone ac supply systems," *IEEE Trans. Ind. Appl.*, vol. 38, no. 2, pp. 533–542, Mar./Apr. 2002.
[21] E. Barklund, N. Pogaku, M. Prodanovic, C. Hernandez-Aramburo, and T. C. Green, "Energy management in autonomous microgrid using stability-constrained droop control of inverters," *IEEE Trans. Power Electron.*, vol. 23, no. 5, pp. 2346–2352, Sep. 2008.
[22] Y. A.-R. I. Mohamed and E. F. El-Saadany, "Adaptive decentralized droop controller to preserve power sharing stability of paralleled inverters in distributed generation microgrids," *IEEE Trans. Power Electron.*, vol. 23, no. 6, pp. 2806–2816, Nov. 2008.
[23] S. V. Iyer, M. N. Belur, and M. C. Chandorkar, "A generalized computational method to determine stability of a multi-inverter microgrid," *IEEE Trans. Power Electron.*, vol. 25, no. 9, pp. 2420–2432, Sep. 2010.
[24] S. G. Mallat, "A theory for multiresolution signal decomposition: The wavelet representation," *IEEE Trans. Pattern Anal. Mach. Intell.*, vol.1, no. 7, pp. 674–693, Jul. 1989.
[25] S. Mallat, "A wavelet tour of signal processing," Academic Press, 1998.

Mojtaba kosari received the B.Sc. degree in electrical engineering from Shiraz University, Fars, Iran, in 2002, and M.Sc. degrees from the Electrical Engineering Department of Amirkabir University of Technology (AUT), Tehran, Iran, in 2004. He is currently pursuing the Ph.D degree in electrical engineering at AUT.

His research interests include distributed generation, microgrid control and applications of power electronics in power distribution systems.

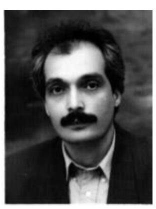

Seyed Hossein Hosseinian was born in Iran in 1961. He received the B.Sc. and M.Sc. degrees from the Electrical Engineering Department of Amirkabir University of Technology (AUT), Tehran, Iran, in 1985, and 1988, respectively, and the Ph.D degree in the Electrical Engineering Department, University of Newcastle, Newcastle Upon Tyne, U.K., in 1995.

Presently, he is a Professor of the Electrical Engineering Department at AUT. His special fields of interest include transient in power systems, power quality, restructuring and deregulation in power systems.